Plant Physiology®

Plant Physiology, 2024, 196, 309–322
https://doi.org/10.1093/plphys/kiae318
Advance access publication 21 June 2024
Research Article

DWARF TILLER1 regulates apical–basal pattern formation and proper orientation of rice embryos

Jingyao Tang,[1] Xiaorong Huang,[2] Mengxiang Sun,[2] and Wanqi Liang[1,3,*]

[1]Joint International Research Laboratory of Metabolic and Developmental Sciences, State Key Laboratory of Hybrid Rice, School of Life Sciences and Biotechnology, Shanghai Jiao Tong University, Shanghai 200240, China
[2]State Key Laboratory of Hybrid Rice, College of Life Sciences, Wuhan University, Wuhan 430072, China
[3]Yazhou Bay Institute of Deepsea Sci-Tech, Shanghai Jiao Tong University, Sanya 572024, China
*Author for correspondence: wqliang@sjtu.edu.cn
The author responsible for distribution of materials integral to the findings presented in this article in accordance with the policy described in the Instructions for Authors (https://academic.oup.com/plphys/pages/General-Instructions) is: Wanqi Liang (wqliang@sjtu.edu.cn).

Abstract

Body axis establishment is one of the earliest patterning events in plant embryogenesis. Asymmetric zygote division is critical for apical–basal axis formation in Arabidopsis (*Arabidopsis thaliana*). However, how the orientation of the cell division plane is regulated and its relation to apical–basal axis establishment and proper position of embryos in grasses remain poorly understood. By characterizing mutants of 3 rice (*Oryza sativa*) *WUSCHEL HOMEOBOX9* (*WOX9*) genes, whose paralogs in Arabidopsis play essential roles in zygotic asymmetric cell division and cell fate determination, we found 2 kinds of independent embryonic defects: topsy-turvy embryos, in which apical–basal axis twists from being parallel to the longitudinal axis of the seed to being perpendicular; and organ-less embryos. In contrast to their Arabidopsis orthologs, OsWOX9s displayed dynamic distribution during embryo development. Both DWT1/OsWOX9A and DWL2/WOX9C play major roles in the apical–basal axis formation and initiation of stem cells. In addition, *DWT1* has a distinct function in regulating the first few embryonic cell divisions to ensure the correct orientation of the embryo in the ovary. In summary, DWT1 acts in 2 steps during rice embryo pattern formation: the initial zygotic division, and with DWL2 to establish the main body axes and stem cell fate 2 to 3 d after pollination.

Introduction

Regular and directional cell division of early embryos is of great importance for most flowering plants, as it controls the formation of body axes, especially the apical–basal axis, essential for later embryo morphogenesis and pattern formation. Organ specialization during embryonic development is accompanied by establishment of overall embryo polarity, leading to differentiation of stem cells in defined regions at specific times. Abnormal division in the early embryo, especially axial changes, often leads to serious defects (Hardtke and Berleth 1998; Hamann et al. 2002; Wu et al. 2007; Armenta-Medina et al. 2017; Zhang et al. 2017a; Jiang et al. 2020).

The current understanding of plant embryonic development is largely based on research conducted in Arabidopsis (*Arabidopsis thaliana*), with its highly ordered, simple, and rigid mode of embryonic cell division and differentiation (Wendrich and Weijers 2013; ten Hove et al. 2015; Palovaara et al. 2016). In Arabidopsis, the formation of the apical–basal axis starts from the initial asymmetrical zygotic cell division, producing a smaller apical cell and a larger basal cell that go on to form the embryo and suspensor initial cells, respectively (Dresselhaus and Jurgens 2021). A mitogen-activated protein kinase (MAPK) cascade containing mitogen-activated protein kinase 6 (MPK6) regulates zygotic division and developmental fate of the basal cell lineage (Lukowitz et al. 2004; Bayer et al. 2009; Ueda et al. 2017; Zhang et al. 2017a). This cascade phosphorylates the transcription factor WRKY DNA-BINDING PROTEIN 2 (WRKY2), which in turn upregulates expression of WUSCHEL-related homeobox transcriptional regulators *WOX8* and *WOX9*, expressed only in basal cells. WOX8/9 non-cell autonomously activate WOX2 expression, essential for the specification of apical cell fate and embryonic shoot patterning (Breuninger et al. 2008). Auxin is also involved in apical–basal axis establishment, and is transported from the basal to the apical cell by the suspensor-specific PIN-FORMED 7 (PIN7) transporters to contributes to proembryo specification together with WOX2 (Friml et al. 2003; Breuninger et al. 2008; Robert Hélène et al. 2013).

Body axis establishment and pattern formation in early grass embryogenesis, such as rice or maize, is much less studied and understood, and appears to be substantially different from the stereotypical pattern of Arabidopsis. Grass early embryo development occurs through oblique cell divisions, with a less predictable cell division pattern, although the first zygote division also produces 2 daughter cells with different sizes. Grass embryos exhibit dorsal–ventral as well as apical–basal polarity, and an endogenous radicle (Sato et al. 1996; Itoh et al. 2005; Chen et al. 2014; Dresselhaus and Jurgens 2021). Furthermore, although key regulators of embryogenesis seem to be conserved in grasses, their expression and functions often diverge from Arabidopsis orthologs, e.g. OsMPK6 is not necessary for asymmetric zygotic division in rice but only for specification of the basal part of embryo (Yi et al. 2016; Ishimoto et al. 2019). In addition, pattern formation and developmental fate determination in the apical and basal cell lineages mediated by WOXs and other conserved regulators appears to occur later in grass embryos than in Arabidopsis,

Received February 23, 2024. Accepted May 10, 2024.

with ZmWOX8/9 expressed at the early transition stage when shoot and root apical meristems are established (Nardmann et al. 2007), while ZmPINs and auxin signals are also not detected until the transition stage (Chen et al. 2014).

WOX8/9 subfamily of the WOX transcription factor gene family has diverse regulatory roles in plant development, including embryo formation, flower development, and somatic embryogenesis. Tomato produces excessive branching of inflorescences due to natural variations in the *WOX8/9* genes or multiple mutations in *WOX8/9* genes (Lippman et al. 2008). In *Petunia hybrida*, the *wox9/evg* mutant produces shoot meristem hyperplasia and fails to produce flowers (Schorderet et al. 2018). Previous studies indicate that *WOX9* has conserved roles in embryonic development in different species, such as tomato (Hendelman et al. 2021) and spruce (Palovaara et al. 2010). Currently no homologs of WOX8 have been identified in monocot genomes but there are 3 *WOX9* orthologs in maize and rice, all of which are expressed during embryogenesis (Nardmann et al. 2007). However, whether they have roles in the embryo development, especially asymmetrical cell division and body axis establishment, is yet unknown.

We have previously identified the rice homolog of *AtWOX9*, *DWT1/WOX9A*, whose mutation causes dwarf tillers (Wang et al. 2014). *DWT1* has 2 homologs in rice—*DWL1/WOX9B* and *DWL2/WOX9C* (Lian et al. 2014)—and we have previously speculated that there might be redundancy between them (Wang et al. 2014; Fang et al. 2020). All 3 genes are expressed in rice embryos, with *DWT1* expression apparent from the zygotic stage (Cheng et al. 2014; Anderson et al. 2017). Here, we demonstrate that the 3 *OsWOX9* genes exhibit some functional redundancy, but that dose effects of *DWT1* and *DWL2* are critical for embryo development. In contrast to AtWOX8/9, DWT1 and DWL2 are not confined to the basal part of embryo, but move dynamically through the embryo during development. Further, *DWT1* appears to have a biphasic role, controlling the overall growth direction of the embryo in the ovule after the zygotic division, and a redundant role with DWL2 in apical–basal axis establishment later in development.

Results

DWT1 displays dynamic distribution during early embryonic development

To define the expression pattern of DWT1 in embryonic development, we complemented the *dwt1-1* line with GFP-tagged DWT1, expressed via its native promoter. The tiller height of regenerated plants recovered, suggesting functional complementation of the mutant phenotype. The distribution of DWT1 signal exhibited dynamic changes at different stages of embryo development. While very weak and evenly distributed in embryonic tissues at 1 d after pollination (DAP; Fig. 1A), DWT1 began to concentrate at the basal region of embryo and maintained a weak signal in the epidermal region by 2 DAP (Fig. 1B). In the transition stage (2 to 3 DAP), DWT1 was observed simultaneously in the basal and shoot apical meristem (SAM) initiation region (Fig. 1C) and by 3 DAP, DWT1 was completely redirected to the SAM initiation region (Fig. 1D). From 4 until 6 DAP, DWT1 was maintained in the SAM and the surrounding leaf primordium (Fig. 1, E to G), after which DWT1 spread to the peripheral vascular bundle and scutellum tissue (Fig. 1, H to K). This result differs significantly from AtWOX9, which remains in the basal region of the embryo (Wu et al. 2007). A previous study shows that the transcripts of *OsWOX9A/DWT1* is evenly distributed in the embryo around 5 DAP (Cheng et al. 2014). We further monitored the spatio-temporal expression pattern of DWT1 at earlier developmental stage by in situ hybridization. We detected the *DWT1* transcripts appearing in the basal region of the embryo from 2 to 4 DAP (Supplementary Fig. S1, A to D). The distribution area of protein signals (Fig. 1, A to C) and mRNA signals deviated after 3 DAP, implicating that DWT1 may act in a non-cell-autonomous manner at the early stage. These results suggest that DWT1 may play varied roles in rice embryonic development to AtWOX9.

Sequence comparison between AtWOX9 and the 3 rice WOX9 proteins revealed high levels of sequence identity in the WOX domain, and that DWT1 and DWL2 are more similar to the Arabidopsis protein than to DWL1, which is substantially shorter than the other rice WOXs (Supplementary Fig. S2A). Further, DWT1 and DWL2 have evolved 2 additional conserved segments absent in AtWOX9, indicating possible functional diversity in rice (motifs 4 and 7; Supplementary Fig. S2B). The distribution of DWL2-eGFP signal during embryonic development closely resembles that of DWT1 (Supplementary Fig. S2, C to F).

Mutations in *OsWOX9* genes result in 2 distinct embryonic abnormalities

To further examine the roles of OsWOX9 proteins, we created single, double, and triple mutants of the 3 *OsWOX9* genes (Supplementary Fig. S3), and monitored embryo development from pollination to 10 DAP (Fig. 2; Supplementary Fig. S4). We could not obtain the *dwt1dwl2* double mutants, suggesting that the double mutant was embryo lethal (Supplementary Table S1); instead, double and triple mutants were generated using heterozygous $DWT1^{+/-}$ or $DWL2^{+/-}$.

At 10 DAP, the wild type (WT) embryo has developed all organs, including the root apical meristem (RAM), SAM, scutellum, and leaf primordia (Fig. 2B; Supplementary Fig. S4D), with apical–basal axis of the embryo (root primordia positioned at the base and shoot primordia positioned at the top) parallel to the longitudinal axis of the seed (Fig. 2B). In mutant lines, endosperms developed normally but there were 2 clearly abnormal embryonic phenotypes: a *topsy-turvy* embryo in which the apical–basal axis being twists from parallel to perpendicular to the longitudinal axis of the seed (named after the topsy-turvy heart, a rare cardiac malformation that involves a 90° clockwise rotation of the heart along its long axis; Fig. 2C; Supplementary Fig. S4, I to L); and an *organ-less* embryo with a dense mass of cells at its center but no apparent organ differentiation (Fig. 2D; Supplementary Fig. S4, M to P). Organ-less embryos do not appear to be a more severe manifestation of topsy-turvy embryos; rather, these 2 phenotypes appear at different stages of embryonic development.

We found no obvious abnormal phenotypes in *dwl2* lines and only ~3% topsy-turvy embryos in *dwl1* lines, a phenotype shared by the double *dwl1dwl2* mutant to Fig. 2A, Supplementary Table S2). In contrast, the *dwt1* single mutant produced ~3% organ-less and ~30% topsy-turvy embryos; adding the *dwl1* mutation generated a slightly higher proportion of topsy-turvy embryos. All $DWT1^{+/-}dwl2$ or $dwt1DWL2^{+/-}$ lines (double or triple mutants) produced 28% to 29% organ-less embryos, with topsy-turvy embryo production in *dwt1* lines at 30% to 34%, and 3% to 5% in $DWT1^{+/-}$ lines (Fig. 2A, Supplementary Table S2). Given the negligible impact of *dwl1* on these more severe phenotypes, and the minor impact of the single mutant, we focused our research on *DWT1* and *DWL2*. Due to the phenotypes of the knockout lines are stable and highly similar among different alleles,

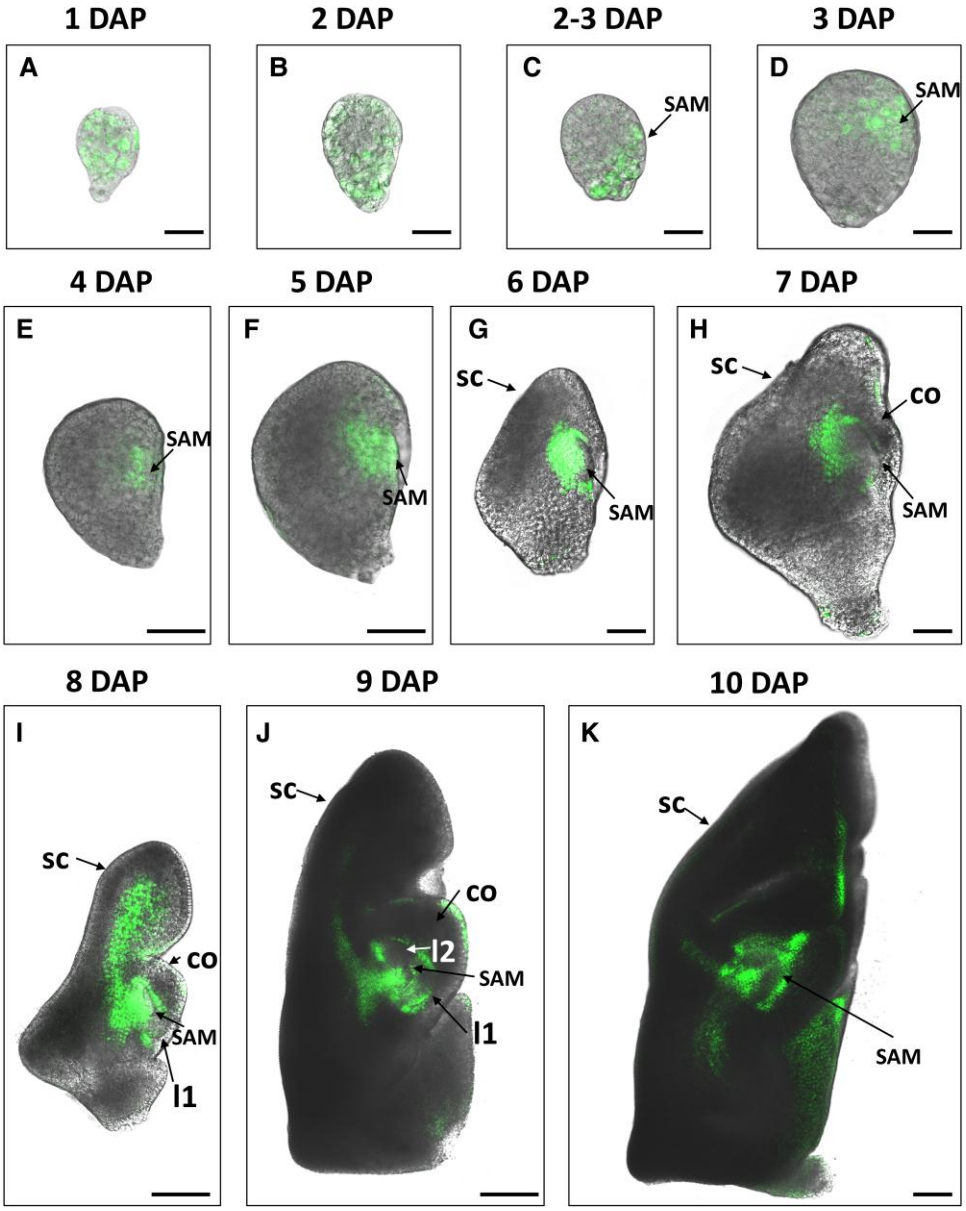

Figure 1. Distribution of DWT1 in embryos from 1 to 10 DAP. **A to G)** DWT1-eGFP signal is uniformly distributed in embryonic tissues at 1 DAP (**A**), and concentrates in the basal area at 2 DAP (**B**). Signal moves to the SAM zone at 2 to 3 DAP (**C, D**), where it remains until 5 to 6 DAP (**F, G**). **H to K)** DWT1 spreads to the leaf primordium, vascular tissue, and scutellum around SAM from 7 DAP. Images show merged fluorescence and bright field from complemented *dwt1* lines expressing GFP-tagged DWT1. co, coleoptile primordium; DAP, day after pollination; l1, l2, leaf primordium 1 or 2; SAM, shoot apical meristem; sc, scutellum. Bars, 25 μm (**A to D**), 50 μm (**E to H**), 100 μm (**I to K**). Images were digitally extracted for comparison.

only *dwt1-l1*, *DWT1*$^{+/-}$*-l1dwl2-l1* (Supplementary Fig. S3) were used in subsequent experiments.

DWT1 and DWL2 affect embryonic apical–basal polarity definition and organ differentiation

Prior to 3 DAP, the organ-less embryos were remarkably similar to WT embryos, demonstrating a normal radial cell division pattern (Fig. 2, E, F, I, and J; Supplementary Fig. S5). The phenotype of organ-less embryos manifests at 4 DAP, when the WT coleoptile primordium starts to differentiate from the globular embryo (Fig. 2, G and H). By contrast, the organ-less embryo retains a dense cell core and keeps expanding evenly in all directions (Fig. 2, J to L). This disordered, near-spherical development occurs through to 10 DAP (Fig. 2D).

The apical–basal axis becomes evident at 2 to 3 DAP in rice (Itoh et al. 2016; Ishimoto et al. 2019). To explore whether apical–basal polarity is normal in organ-less embryos, we selected 4 marker genes that define either the basal (*ZFN1* and *ACO1*) or apical (*ERECTA* and *PIP2*) regions of the embryo at 3 DAP (Itoh et al. 2016; Ishimoto et al. 2019). In the *DWT1*$^{+/-}$*dwl2* ovaries, ~28% embryos showed no apical or basal marker gene expression (Fig. 3, A to H), which corresponds to the expected proportion of organ-less embryos in double mutants, suggesting that DWT1 and DWL2 are indispensable for the formation of this basic axis.

We used a further 4 marker genes expressed in specific regions of the embryo to explore the development of polarity and determination of cell fate within the organ-less embryo: HD-ZIP IV homeobox gene *ROC1*, which is specifically expressed in the epidermis (Ito et al. 2002); *OsWOX5*, which is weakly but

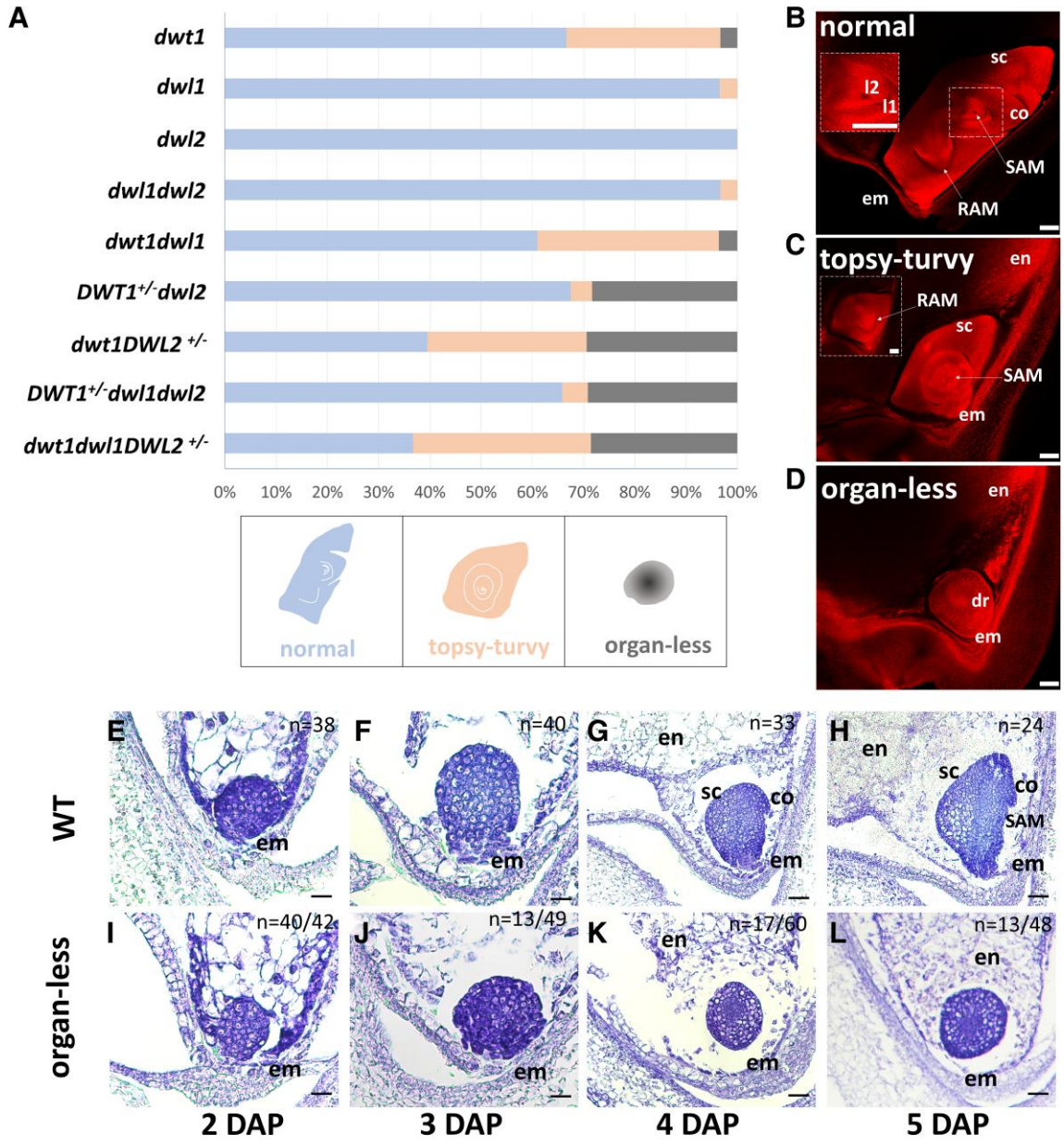

Figure 2. Embryonic phenotypes of *OsWOX9* clade mutants. **A)** Schematic diagram of embryonic phenotypes of single, double, and triple *OsWOX9* mutants. See also Supplementary Table S2. **B to D)** Phenotypes at 10 DAP of normal (**B**), topsy-turvy (**C**), and organ-less (**D**) embryos. The plane of the topsy-turvy embryo's root primordium is depicted in the dotted box, positioned behind the SAM. **E to L)** Longitudinal sections of wild type (WT, **E to H**) and organ-less (*DWT1*$^{+/-}$*dwl2*, **I to L**) embryos at 2 to 5 DAP. The upper right corner shows the number of samples assessed, with the abnormal fraction given in mutant panels. co, coleoptile primordium; DAP, day after pollination; dr, disordered region; em, embryo; en, endosperm; l1, l2, leaf primordium 1 or 2; RAM, root apical meristem; SAM, shoot apical meristem; sc, scutellum; WT, wild type. Bars, 125 μm (**B to D**), 12.5 μm (**E, F, I, J**), 25 μm (**G, H, K, L**).

specifically expressed in the quiescent center region of the embryonic root apical meristem (Kamiya et al. 2003). *SCR*, which is specifically localized in the endodermis of the embryo (Sazuka et al. 2009); and *OsPNH1*, which is expressed in the future vascular region of rice embryos (Nishimura et al. 2002; Yi et al. 2016). These markers were used for in situ hybridization in 5 to 6 DAP organ-less embryos, revealing that epidermal and provascular region markers were present, albeit substantially decreased compared with WT (Fig. 3, M and N), but that no quiescent center or endodermis markers were detected (Fig. 3, O and P).

It has been well documented that polarized, dynamic auxin distribution plays an essential role in Arabidopsis embryo fate establishment and pattern formation (Armenta-Medina and Gillmor 2019). We used DR5-VENUS auxin reporter lines to examine the impact of *WOX9* mutations on auxin dynamics in WT and organ-less rice embryos. Auxin distribution in maize embryos has been reported to be markedly distinct from Arabidopsis with the earliest auxin response inside the embryo detectable relatively late in development (~8 DAP) (Moller and Weijers 2009; Chen et al. 2014). By contrast, we observed that the auxin signal appears very early (~1 DAP, 32-cell stage) and remains evenly distributed before 3 DAP (Supplementary Fig. S6, A to C). From late 3 DAP, there is a significant shift, with the signal disappearing from the ventral SAM region, but accumulating in the RAM initiation and apical regions (Supplementary Fig. S6, D and E). Weak auxin signals also accumulated at the tip of the leaf primordium and vascular tissue from 5 to 10 DAP (Supplementary Fig. S6, F to K). These results suggest that proper auxin distribution may be

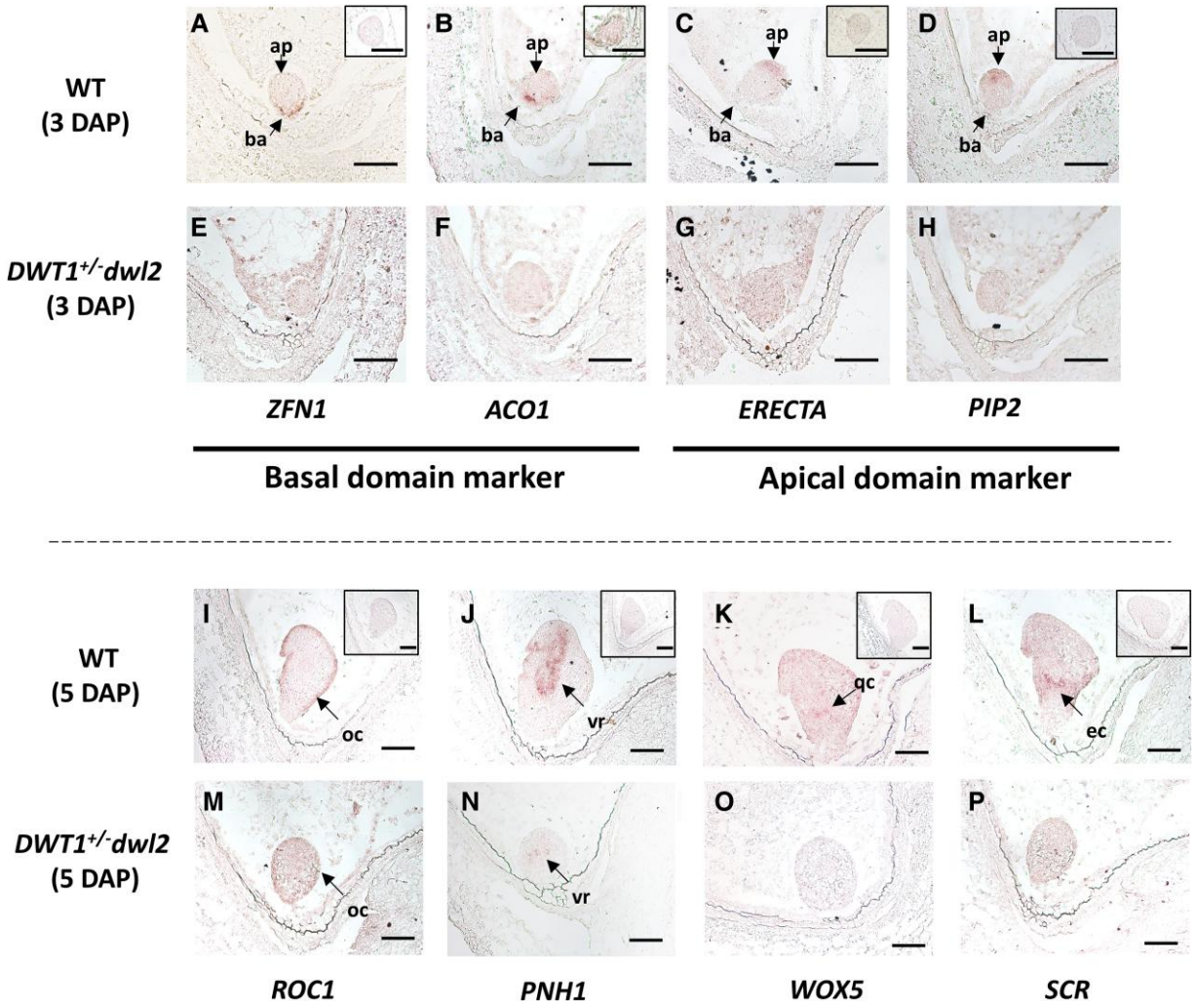

Figure 3. Molecular analysis of the organ-less embryo. **A to H)** In situ hybridization in 3 DAP WT and organ-less embryos of basal region-specific marker genes *zinc finger nuclease 1* (*ZFN1*; **A, E**) and *ACC oxidase 1* (*ACO1*; **B, F**); and apical region-specific marker genes *ERECTA-like kinase 1* (**C, G**) and *piriformospora indica-insensitive protein 2* (*PIP2*; **D, H**). **I to P)** RNA in situ hybridization of *ROC1* (**I, M**), *PNH1* (**J, N**), *WOX5* (**K, O**), *SCR* (**L, P**) at 5 DAP in WT and *DWT1*$^{+/-}$*dwl2* embryos. *ROC1* and *PNH1* signals were detected in the mutant (**M, N**); while *WOX5* and *SCR* signals disappear completely (**O, P**). The black box in the upper right corner of WT images shows hybridization with the corresponding sense probe. ap, apical region; ba, basal region; DAP, day after pollination; ec, endodermis cell layer; qc, quiescent center; oc, outermost cell layer; vr, provascular region; WT, wild type. Bars, 50 μm.

essential for establishing apical–basal and dorsal–ventral polarity as well as SAM/RAM initiation in rice embryos. In the organ-less embryo, the auxin signals remained uniformly distributed, similar to WT, until early 3 DAP (Supplementary Fig. S6, L to N). After this stage, however, the auxin signal maintained a uniform distribution in the central region of the embryo (Supplementary Fig. S6, O to T), leading to the loss of polarity guidance for embryonic cell development. These observations indicate that the normal WOX9 function is required for polarized auxin distribution during embryo development in rice.

We conclude that the organ-less embryo has completely lost its apical–basal polarity, leading to disordered division with inner cells unable to complete their fate transition into specific organs.

DWT1/DWL2 is required for shoot and root meristem initiation

DWT1 and DWL2 specifically accumulate in the future SAM region from 3 DAP, suggesting that they may be directly involved in the SAM formation (Fig. 1, Supplementary Fig. S2, C to F). *OSH1* (*Oryza sativa* homeobox 1), a marker for SAM (Sato et al. 1996), was not detected in 3 DAP organ-less embryos (Supplementary Fig. S7, A and D), indicating that SAM formation of organ-less embryos fails during this transitional period.

We further examined the expression of genes critical for meristem cell fate decision. In Arabidopsis, transcription factors HD-ZIP III and PLETHORA (PLT) determine shoot and root characteristics, respectively, in an antagonistic manner. The *PLT* family has 11 members in rice (Li and Xue 2011), the triple mutant of *bbm1bbm2bbm3* (*plt6/plt3/plt5*) exhibits abnormal embryo development (Khanday et al. 2019). The HD-ZIP III family has 5 rice homologs, *OsHB1–5*, whose expression has been detected in the embryo as in Arabidopsis (Roodbarkelari and Groot 2017; Zhang et al. 2017b), but no embryonic mutants have been reported. *OsHB1, 3, 4* is strongly expressed in the SAM and central vascular region (Itoh et al. 2008).

We analyzed the expression of these genes at 3 and 5 DAP by in situ hybridization (Fig. 4). *OsHB1, 3, 4* at 3 DAP were expressed in similar regions in WT and organ-less embryos, albeit at much lower levels in the mutant (Fig. 4, A to C and E to G). By 5 DAP, the WT

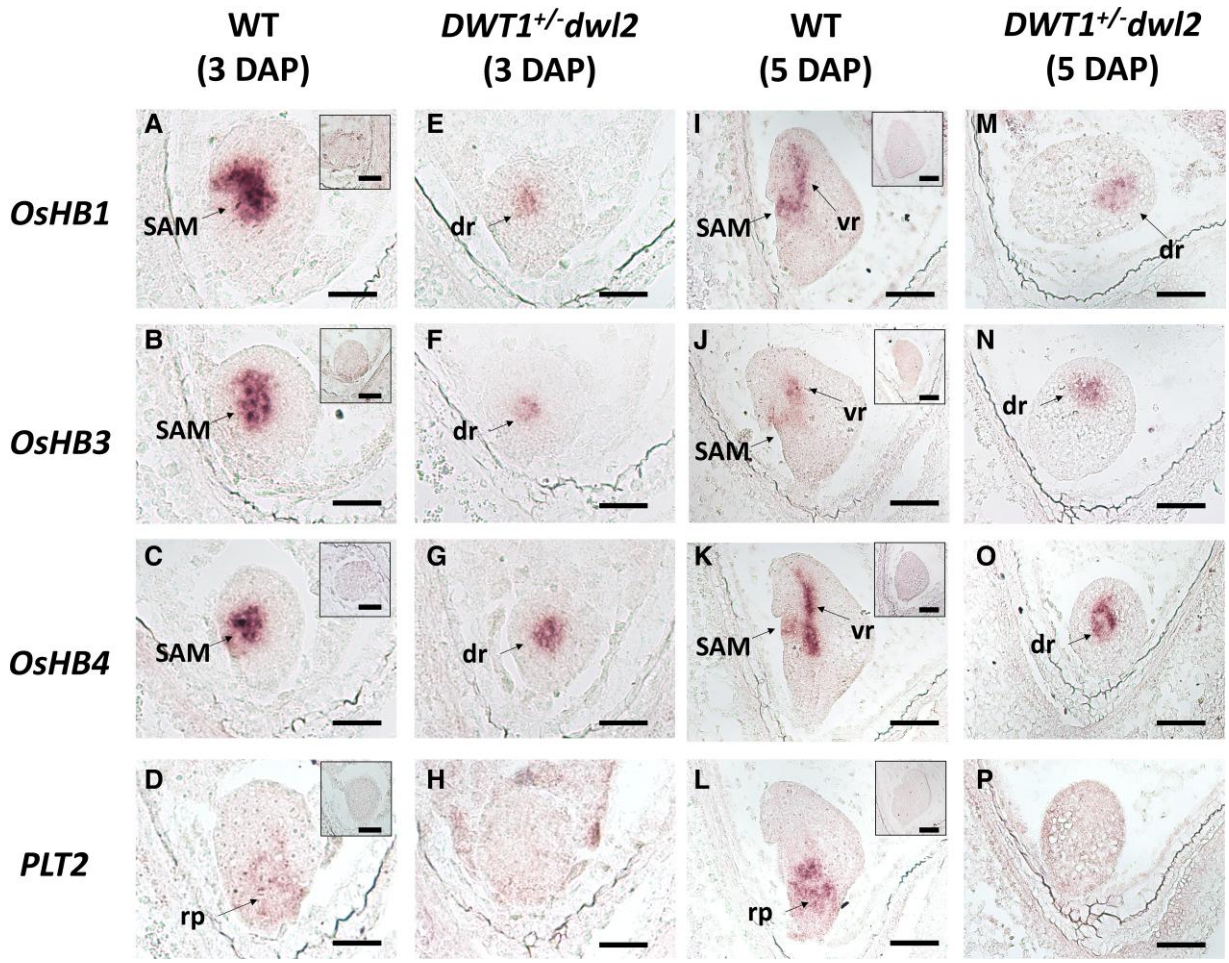

Figure 4. Expression of *HD-ZIP III* and *PLETHORA* genes in organ-less embryos. **A to P)** In situ hybridization of *OsHB1*, *OsHB3*, *OsHB4*, and *PLT2* in WT and organ-less embryos at 3 DAP (**A to H**) and 5 DAP (**I to P**). *OSHB1, 3, 4* exhibited similar expression patterns, with signal distribution observed in the stem tip meristem and vascular bundle in WT (**A to C, I to K**), but the central region of the mutant embryo (**E to G, M to O**). *PLT2* signal was distributed in the basal region of WT embryos (**D, L**) but completely undetectable in mutant embryos (**H, P**). The black box in the upper right corner of WT images shows hybridization with the corresponding sense probe. DAP, day after pollination; dr, disordered region; rp, root primordia; sa, shoot apical meristem; vr, provascular region; WT, wild type. Bars, 25 μm (**A to H**), 50 μm (**I to P**).

signal decreased to similar levels as the mutant, but exhibited a clear distribution pattern into the SAM and vascular bundle region that was absent in the mutant (Fig. 4, I to K and M to O). Of the *PLT* genes, only *PLT2* had specific localization in the basal region in WT embryos (Fig. 4, D and L), with no expression of *PLT2*, *PLT1*, or *PLT6* (*BBM1*) detected in mutant embryos at either timepoint (Fig. 4, H and P; Supplementary Fig. S7, B, C, E, and F).

The topsy-turvy phenotype manifests with the first few divisions of embryogenesis

We used CT scans to further understand the topsy-turvy abnormality using *dwt1-l2* lines. The overall direction of the topsy-turvy embryo is deflected laterally at seed maturity, with the shoot and root domain twisted from the WT up–down relationship to a horizontal alignment (Fig. 5, A to L), in line with our clearing results at 10 DAP (Fig. 2C) and maturity (Supplementary Fig. S8, A to D). This twisting is demonstrated clearly in Supplementary Videos S1 (WT) and S2 (topsy-turvy). Through extensive observation of *dwt1* embryos, it was noted that 30% exhibited a "flat" phenotype at 2 to 3 DAP, which were dramatically flatter with a significantly shorter longitudinal axis than WT embryos (Fig. 5, M and Q). This flat embryo phenotype was rarely observed in *DWT1*$^{+/-}$*dwl2* (organ-less) or WT lines, suggesting that the flat embryo may represent an early form of the topsy-turvy embryo. Indeed, the continuity of morphological changes from flat to topsy-turvy embryos can be observed through 3 to 5 DAP (Fig. 5, R to T). The transverse: longitudinal axis length ratio in topsy-turvy embryos was significantly higher than WT at each period (Fig. 5U), indicating that initiation of the topsy-turvy phenotype occurs prior to 2 DAP.

Previous studies indicate that in rice, the first zygote division occurs obliquely, producing a smaller upper cell and a larger lower cell similar to that in Arabidopsis. While several other embryonic mutants have been reported in rice, these mutants exhibit normal cell division pattern before organ differentiation (Nagasaki et al. 2007; Huang et al. 2017; Ishimoto et al. 2019), suggesting that they are not involved in very early pattern formation. In Arabidopsis, WOX8/9 and WOX2 play essential roles in establishing the apical and basal cell identities after the first zygote division. To explore whether *WOX9* genes are also required for the early pattern formation in rice, we examined WT, topsy-turvy (*dwt1*), and organ-less (*DWT1*$^{+/-}$*dwl2*) rice ovaries at 6 to 30 h after pollination to analyze embryo structure from the zygote to the 32-cell stage (Fig. 6, A to F and H to M; Supplementary Fig. S9).

The WT zygote divides obliquely, with the upper and lower daughter cells forming a vertical apical–basal axis (Fig. 6, B and

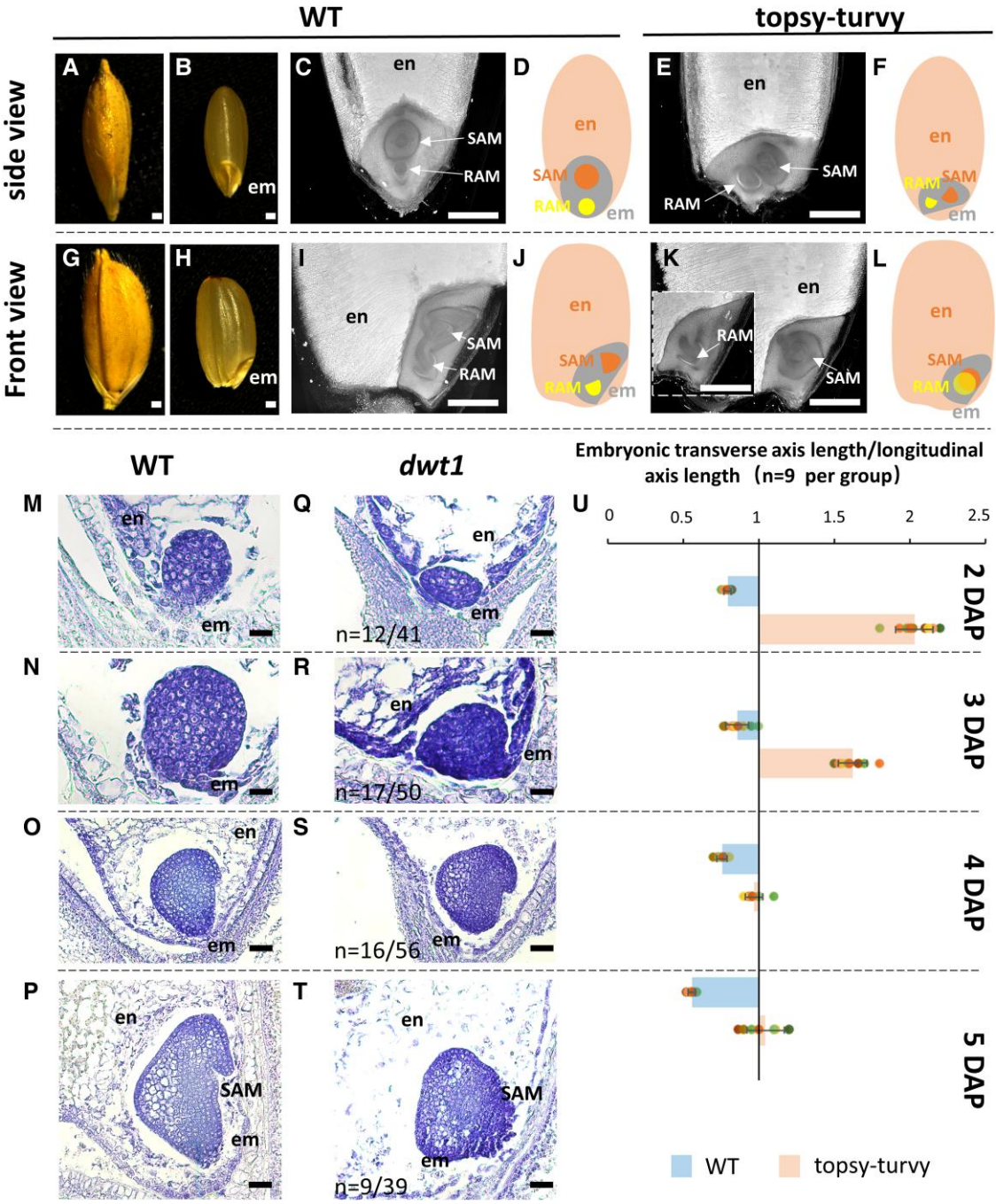

Figure 5. Morphological analysis of topsy-turvy (*dwt1*) embryos. **A to L)** Front and side views of WT (**A to D, G to J**) and topsy-turvy (**E, F, K, L**) rice seeds. **A, G)** Seed with husk. **B, H)** Seed without husk. **C, E, I, K)** Computed tomography (CT) scan. The plane of the topsy-turvy embryo's root primordium is shown in the dotted box, located behind the SAM (**K**). **D, F, J, L)** Schematic representation of the embryo, showing the endosperm (en), embryo (em), shoot apical meristem (SAM), and root apical meristem (RAM). **M to T)** Longitudinal sections of WT (**M to P**) and topsy-turvy (**Q to T**) embryos at 2 DAP (**M, Q**), 3 DAP (**N, R**), 4 DAP (**O, S**), and 5 DAP (**P, T**). The bottom left corner shows the number of samples assessed, with the abnormal fraction given in mutant panels. **U)** Ratio of transverse: longitudinal axis length of WT and topsy-turvy embryos at 2 to 5 DAP. Data show mean ± SD ($n = 9$), dots show each individual result. DAP, day after pollination; WT, wild type. Bars, 500 μm (**A to K**), 12.5 μm (**M, N, Q, R**), 25 μm (**O, P, S, T**).

O). Subsequently, the 2-cell proembryo divides vertically or obliquely to the first division plane (Fig. 6C). In contrast, ~17% *dwt1* embryos showed irregularities after the first zygotic division, with abnormal cell expansion resulting in bending of the apical–basal axis (Fig. 6, I and P) and one of the 2 daughter cells dividing parallel to the previous plane of division (Fig. 6J). Changes in the overall growth direction accumulate and intensify from the first division, leading to the overall growth of the axis changing from longitudinal to transverse, producing a flattened embryo at 2 DAP (Fig. 6, K to N and R). These changes are most pronounced at the 16 to 32-cell period to Fig. 6, L and M).

In situ hybridization of polarity marker genes at 3 DAP was used to validate the distortion of topsy-turvy embryos during early growth by selecting "flat" embryos for mutant analysis. As

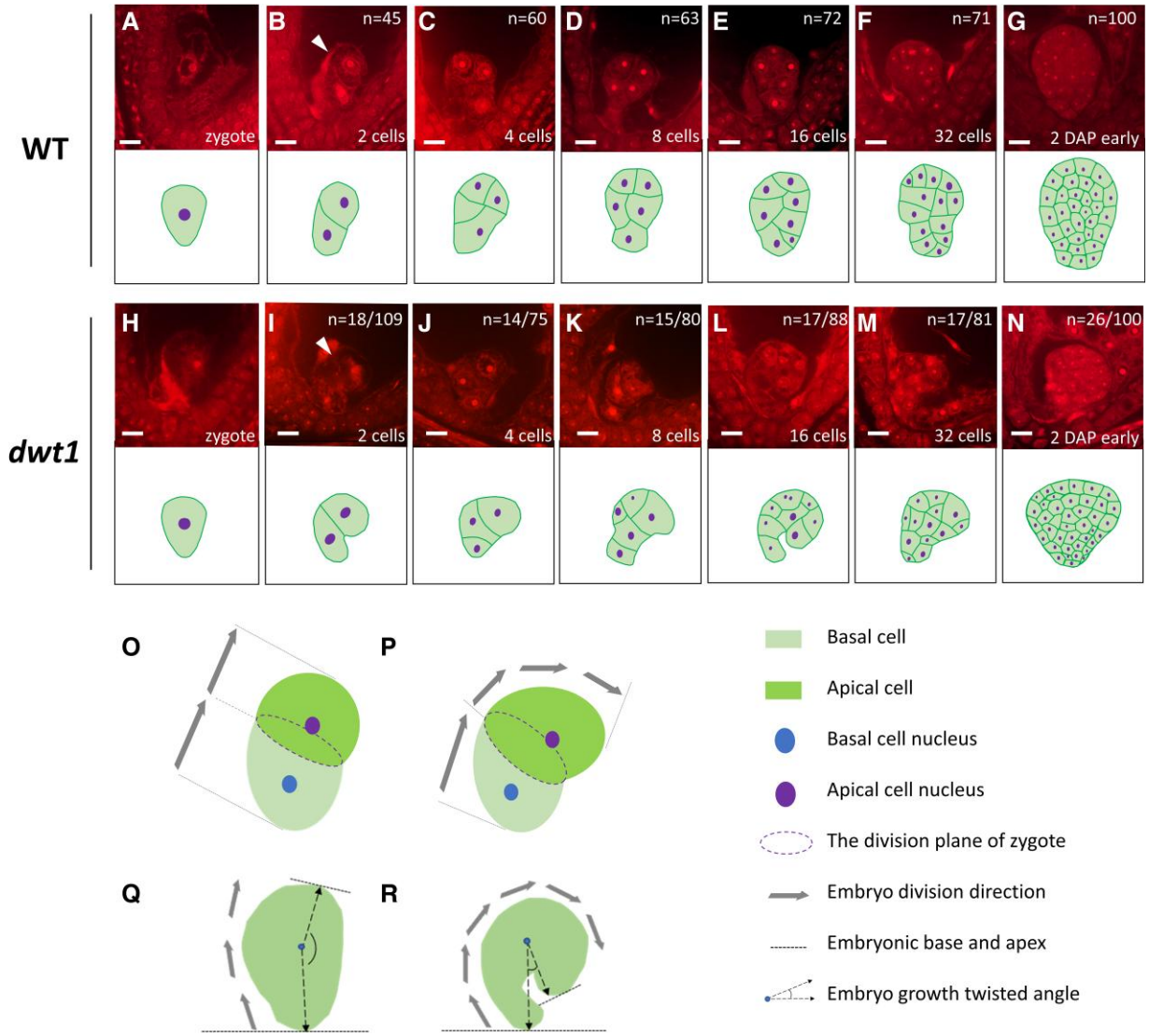

Figure 6. Cell division in *dwt1* embryos at 1 to 2 DAP. **A to N)** Clear staining of WT (**A to G**) and *dwt1* topsy-turvy (**H to N**) embryos from the zygote stage to 2 DAP, with corresponding schematic representations given in below. The upper right corner shows the number of samples assessed, with the abnormal fraction given in mutant panels. The white arrowhead (**B, I**) marks the position of the zygotic splitting plane. DAP, day after pollination; WT, wild type. Bars, 12.5 μm. **O, P)** Schematic representation of the first division in WT (**O**) and topsy-turvy (**P**) zygotes. **Q, R)** Schematic diagram of the twisting angle at the 16 to 32-cell stage of WT (**Q**) and topsy-turvy (**R**) embryos.

expected, apical–basal polarity signals were detected in topsy-turvy embryos, but at different positions relative to WT embryos. For example, *ACO1* and *PIP2/ERECTA* signals extend and shift beyond the basal and apical regions of WT embryos, respectively (Fig. 7, D to F and H to J); while the *ZFN1* signal appears to have no clear polarity distribution through the entire embryo cross-section (Fig. 7, C and G). The *OSH1* signal (SAM marker) was present in an expected but in a much narrower region, indicating that cell differentiation and organ formation had begun by 3 DAP, as in WT embryos (Fig. 7, A and B), but were obviously modified.

The topsy-turvy embryos showed overall normal morphology and organ differentiation at maturity (Supplementary Fig. S8, A to D). To explore whether the change in embryo orientation affects post-embryonic growth, we compared seed germination and seedling growth of WT and *dwt1* plants. We observed ~28% of mutant seeds exhibited much delayed germination or could not germinate. After removed the husk, we observed that these seeds produced only roots or shoots, deformed roots and shoots at the fifth day after soaking (Supplementary Fig. S8, E to L; Supplementary Table S3), which aligns with the expected proportion of topsy-turvy embryos (cf. Figure 2A; Supplementary Table S2). Although most of distorted seedlings could grow normally later except for ~10% seedling lethal, we proposed that a delayed germination and distorted outgrowth will affect the survival rate and the growth vigor of mutant plants under a harsh field condition. These observations suggest that the correct orientation of embryo in the ovary is important for normal seed germination and post-embryonic organ development.

Discussion

WOX8/9 are the founding members of the intermediate subclade of the homeodomain WOX transcription factor gene family; in Arabidopsis, their roles in mediating zygote asymmetric cell division and apical–basal polarity establishment are well known. The functions of orthologous proteins in grasses during embryogenesis are less well understood, although they are known to be highly

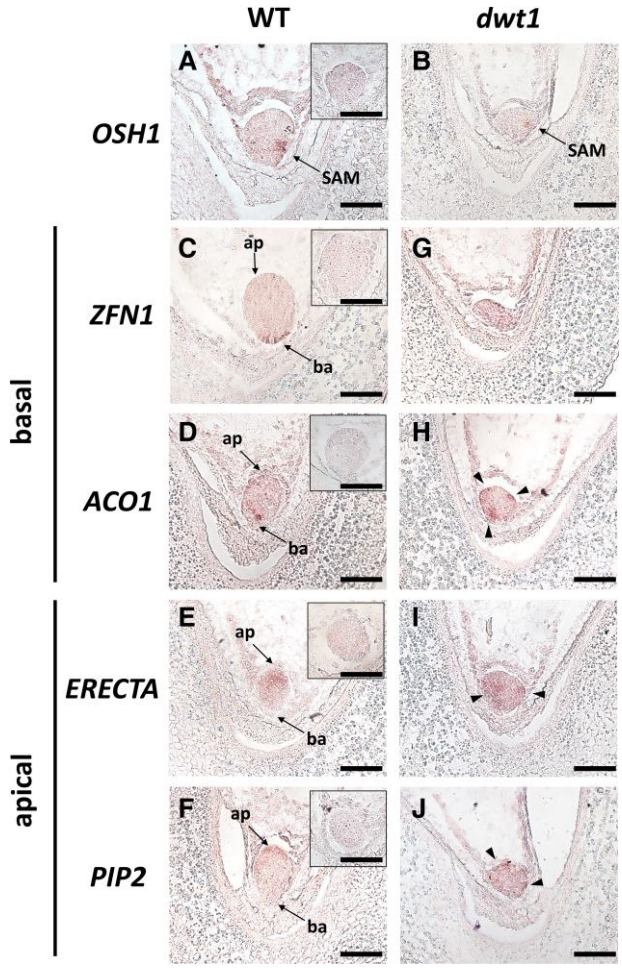

Figure 7. Molecular analysis of topsy-turvy (*dwt1*) embryos at 3 DAP. **A, B)** RNA in situ hybridization of *OSH1*, with signals detected in WT (**A**) and topsy-turvy (**B**) embryos. **C to J)** In situ hybridization of basal- or apical-specific marker genes *ZFN1* (**C, G**), *ACO1* (**D, H**), *ERECTA* (**E, I**), and *PIP2* (**F, J**) in WT and topsy-turvy embryos. The black box in the upper right corner of WT images shows hybridization with the corresponding sense probe. Black arrowheads indicate the location of the signal (**H, I, J**). ap, apical region; ba, basal region; SAM, shoot apical meristem; WT, wild type. Bars, 50 μm.

expressed during embryonic development (Nardmann et al. 2007). Here, we observed substantial functional redundancy between the 3 *OsWOX9* genes, with 2 main genes (*DWT1* and *DWL2*) demonstrating essential roles in regulating embryonic development.

In Arabidopsis, it is well documented that the asymmetric zygote cell division plays an indispensable role in body axis establishment. In grass embryos, the cell division plane and pattern are very different from that of Arabidopsis. The zygote undergoes oblique rather than horizontal cell division, and cell vision pattern of its descendants is less regular and predictable when compared with Arabidopsis. In rice, although zygote division also produces 2 daughter cells of different size, whether this step is essential for the following apical–basal pattern formation and how this step is regulated remain largely unknown. Here, we reveal that the homeodomain WOX transcription factors WOX9s regulate the early cell division and body axis formation in rice.

In Arabidopsis, *AtWOX8/9* are essential for the development of basal and apical embryonic lineages as early as the 2-cell stage, with expression confined to the basal cell lineage (Wu et al. 2007; Breuninger et al. 2008). Previous studies report a similar expression pattern of *WOX9* genes in the rice embryo: transcriptome analysis revealed that *DWT1/OsWOX9A* is induced in the zygote shortly after fertilization (Anderson et al. 2017), while expression of *OsWOX9A/B* was not detectable using RT-qPCR until 3 DAP, predominantly in the basal part of the embryo (Itoh et al. 2016; Ishimoto et al. 2019). This is consistent with the in situ hybridization results of *DWT1* shown in this study (Supplementary Fig. S1C). By contrast, we observed a dynamic and much longer-lasting DWT1 and DWL2 presence in the developing rice embryo (Fig. 1; Fig. 8A; Supplementary Fig. S2, C to F). The GFP signal in the DWT1-GFP lines first appeared around 1 DAP (~32-cell embryo). The signal was initially evenly distributed, then became more focused in the basal part at 2 DAP, suggesting that they may be directly involved in the specification of basal embryo characteristics. At the transition stage (2 to 3 DAP), DWT1 was redirected to the future SAM region and subsequently observed in meristem cells. After 5 DAP, DWT1 diffuses into the leaf primordium, vascular, and scutellum tissue (Fig. 1, G to K), where it may subsequently regulate development of peripheral tissues such as young leaves. These observations suggest that DWT1 and DWL2 (with its similar expression pattern) may have pleotropic functions at different embryonic stages; further, the difference in the transcript and protein level suggests that DWT1/DWL2 may act non-cell autonomously.

Consistent with the dynamic distribution pattern, 2 abnormal embryonic phenotypes were observed in single, double, and triple *oswox9* mutants: topsy-turvy embryos, caused mainly by *dwt1* mutation, developed abnormalities from the first zygotic division, but could still differentiate normally and germinate successfully; while organ-less embryos, caused by the double *dwt1 dwl2* mutations, developed abnormalities from 3 DAP and did not produce viable embryos (Fig. 8). We speculate that rice embryogenesis may be a phased process, with DWT1 involved in 2 regulatory pathways before and after 2 to 3 DAP.

Organ-less embryos completely failed to develop apical–basal characteristics (Fig. 3), but initiate cell differentiation as well as organ formation by 3 DAP (Fig. 2). Outer cells still express the epithelial marker *ROC1* (Fig. 3M) and the inner cells are still capable of expressing the provasculature marker *PNH1* (Fig. 3N), indicating that the initial radial polarity information is maintained in the mutant embryo. Several genes specifically expressed in the basal part after 3 DAP, including *OsWOX5*, *SCR*, and *PLT2*, were not expressed in the organ-less embryos (Fig. 3, O and P; Fig. 4, H and P). Similar to the *osmpk6/gle4* mutant that is also defective in apical–basal polarity (Ishimoto et al. 2019), asymmetric zygotic cell division was not visibly affected in the *dwt1dwl2* organ-less embryos. These results suggest that DWT1/DWL2 may play a conserved role in the basal pattern formation, but at a much later developmental stage than Arabidopsis. *OsWOX2* is not expressed in the embryo but in the endosperm (Wang et al. 2018), and future research will investigate whether OsWOX2 is involved in embryogenesis and apical cell fate determination in rice, and whether DWT1/DWL2 have a regulatory role in this process.

Auxin plays a major role in embryo fate establishment in Arabidopsis but, again, relatively little is known of auxin's role in grass embryo axis formation. Our results show that auxin distribution is dynamically regulated during rice embryo development. At 3 DAP during SAM emergence and organ specialization, auxin signals change from a uniformly distributed pattern to an apical–basal tip accumulation pattern (Supplementary Fig. S6). DWT1 appears to condense in the SAM earlier than auxin moves to the poles, and by late 3 DAP, the distribution of DWT1 is complementary to that of auxin (Fig. 1D; Supplementary Fig. S6D). Auxin redistribution is

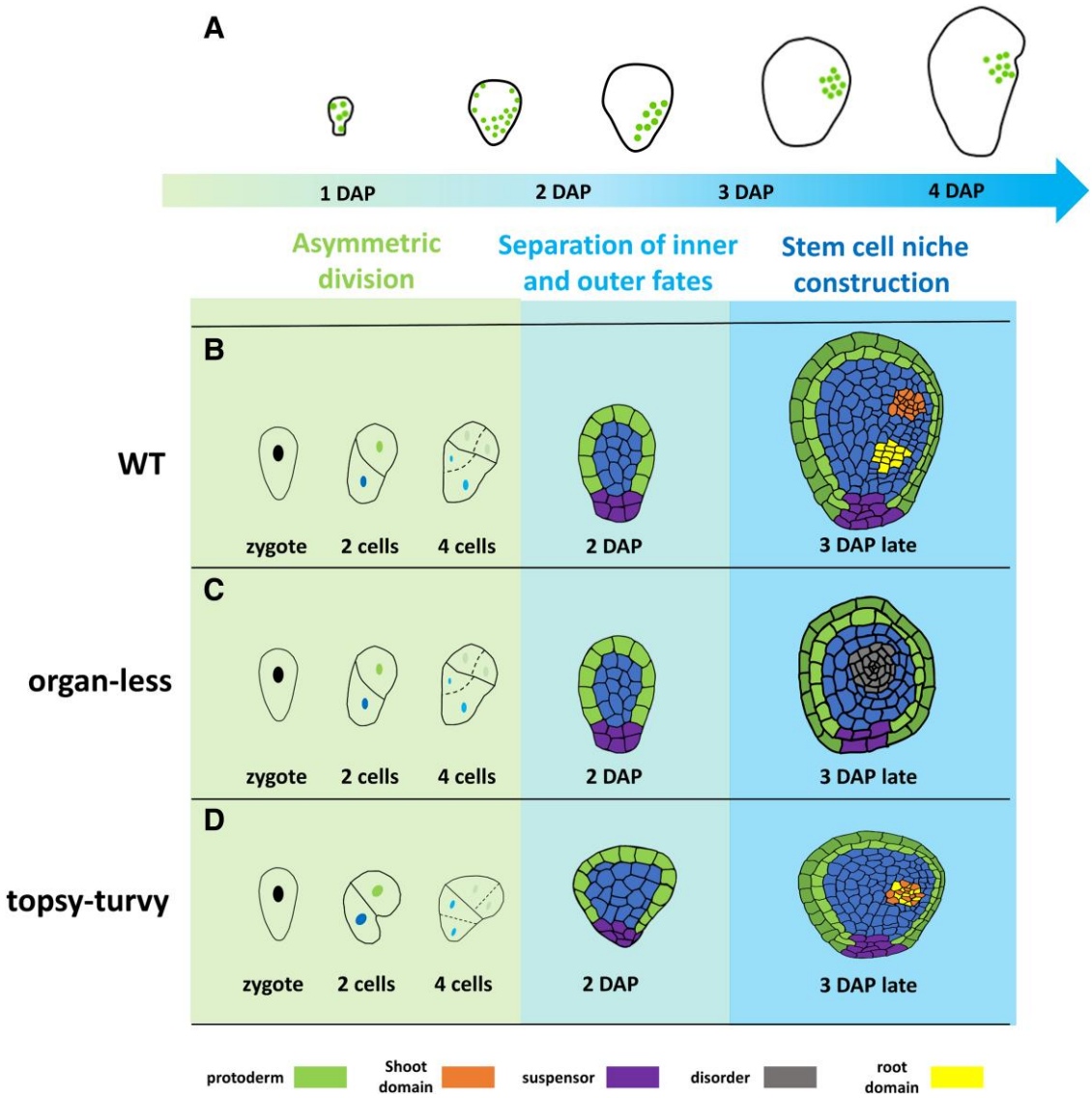

Figure 8. Proposed model of *WOX9* action. **A)** Schematic diagram of DWT1 location during early embryonic development. The line depicts the embryo outline, and the dots represent DWT1-eGFP protein signal (cf. Figure 1). **B to D)** Schematic diagram of 3 phenotypes during the early division of rice embryos. DAP, day after pollination; WT, wild type.

disrupted in the organ-less embryo (Supplementary Fig. S6), similar to that in the *wox8wox9* double mutant, indicating a conserved role in controlling auxin localization.

The concentration of DWT1 and DWL2 in the future SAM position at 3 DAP (Fig. 1D; Supplementary Fig. S2C) suggests that OsWOX9 proteins are involved in stem cell niche formation. In Arabidopsis, SAM and RAM initiation is driven by HD-ZIP III and PLT transcription factors, respectively (Aida et al. 2004; Prigge et al. 2005; Smith and Long 2010). In organ-less embryos, *HD-ZIP III* (*OsHB1, 3, 4*) signals were substantially decreased in the presumed SAM region (Fig. 4, E to G and M to O); and no *PLT* or *OSH1* signals were detected (Fig. 4, H and P; Supplementary Fig. S7D). As PLT proteins are auxin-dependent transcription factors (Palovaara et al. 2016), the lack of *PLT* expression may be explained by the abnormal auxin distribution in mutant embryos (Supplementary Fig. S6). The effect of HD-ZIP III may be more complex. Previous research has suggested that HD-ZIP III can impact auxin distribution by influencing PIN auxin transporters (Izhaki and Bowman 2007; Itoh et al. 2008; Zhang et al. 2017b), and may inhibit the distribution of auxin in the SAM initiation region (Zhang et al. 2017b). Auxin and transcription factors are 2 major components in plant embryo development, both of which are affected in organ-less embryos leading to defects in stem cell initiation.

Current dogma suggests that while the first division of grass zygote is asymmetric, subsequent divisions are frequently less regular and predictable (Dresselhaus and Jurgens 2021). Our investigation into topsy-turvy embryos reveals that cell divisions following zygotic division in rice are also tightly regulated. We demonstrated that DWT1 can influence the cell expansion and subsequent division pattern of zygotic daughter cells, while DWL1 might have a minimal role in this process (Fig. 2; Fig. 6). Although the DWT1-GFP signal is hard to be detect in the zygote and embryos prior to the 16-cell stage, it is likely that a low level of DWT1 is sufficient to regulate early embryonic cell division (Fig. 1A; Fig. 8A). However, the severe abnormality of topsy-turvy embryos prior to 2 DAP does not inhibit major embryonic structure differentiation (Fig. 5), or preclude germination (Supplementary Fig. S8, F to J). We propose that, in rice, the direction of first few

cell divisions during early embryogenesis may not be intimately associated with apical–basal axis establishment. However, the change in the overall growth direction affects organ development after seed germination, which may explain why the growth direction is under stringent control.

We conclude that *DWT1* is the primary gene in the *OsWOX9* clade that regulates rice embryonic development, showing temporal dynamic characteristics before and after 2 DAP. *DWT1* can influence the direction of the first division of zygotes and subsequently impact overall embryonic growth direction, while *DWL1* has a minimal redundant role in this process (Fig. 8D). Furthermore, *DWT1* collaborates with *DWL2* to establish the apical–basal axis and meristem cell fate by influencing the expression of several key transcription regulators at 2 to 3 DAP, and coordinating the gradient of auxin distribution (Fig. 8C) essential for embryo morphogenesis and organ formation. The dynamic distribution of DWT1 and its distinct roles in 2 developmental stages differ significantly from *AtWOX8/9* (Wu et al. 2007; Breuninger et al. 2008). Our study provides insights into the mechanism underlining the grass embryo development, especially into early cell division pattern control.

Materials and methods

Plant materials and growth conditions

All rice (*Oryza sativa*) plants (cultivar '9522' as wild type [WT]) used in this study were grown in the paddy field of Shanghai Jiao Tong University from June to September, with embryos harvested from mid- to late September. DR5-VENUS auxin reporter lines were obtained from Yang et al. (2017).

Mutant generation

dwt1-l2 was isolated from our rice mutant library (Wang et al. 2014). We created 2 more alleles of *dwt1*, 3 alleles of *dwl1*, and 4 alleles of *dwl2* via CRISPR/Cas9 technology as described (Zhang et al. 2014). The sgRNA sequences are listed in Supplementary Table S4. We further created double and triple mutants by crossing, finally obtaining 12 double mutants 12 double mutants *dwt1-1DWL2*$^{+/-}$-1/2, *dwt1-1DWL2*$^{+/-}$-4, *DWT1*$^{+/-}$-*1dwl2-1/2*, *DWT1*$^{+/-}$-*1dwl2-4*, *DWT1*$^{+/-}$-*1dwl2-5*, *dwt1-1dwl2-3* (weak allele of *DWL2*), *dwl1-3dwl2-5*, *dwl1-3dwl2-4*, *dwt1-1dwl1-2*, *dwt1-1dwl1-3*; and 2 triple mutants *DWT1*$^{+/-}$-*2dwl1-3dwl2-4*, *dwt1-1dwl1-3DWL2*$^{+/-}$-5.

The *dwt1-1* and DR5-VENUS lines were hybridized in the T_2 generation to obtain the *dwt1-1* auxin reporter line, which was subsequently crossed with the *dwl2-1/2/4* line to obtain the DR5-VENUS reporter in the *DWT1*$^{+/-}$*dwl2* background.

For complementation lines, the *proDWT1::DWT1–eGFP* construct was generated by inserting the full-length *DWT1* gDNA fragment with eGFP (enhanced green fluorescent protein) into the *Bam*HI and *Bgl*II sites of pCAMBIA1301 using In-Fusion (Takara) cloning technology. This construct was introduced into *dwt1-1* calli via Agrobacterium (*Agrobacterium tumefaciens*)-mediated transformation (Hiei et al. 1994). The same operation was used for the *proDWl2::DWl2–eGFP* construct, using the *Kpn*I and *Spe*I sites of pCAMBIA1301, and introduced into *dwt1-1DWL2*$^{+/-}$-*1* calli. Primers for cloning and vector construction are given in Supplementary Table S4.

Bioinformatic analysis of the rice WOX9 subfamily

The full-length amino acid sequences of WOX9 proteins were downloaded from Phytozome (Plant Comparative Genomics portal of the Department of Energy's Joint Genome Institute, https://phytozome-next.jgi.doe.gov/), and aligned using Snap gene software (https://www.snapgene.com). Protein motif search, alignment, and consensus sequence determination were performed using the analysis tool from https://meme-suite.org/meme/index.html in Classic mode.

Phenotypic observation

Embryo development was monitored by wholemount eosin B-staining confocal microscopy as described by Huang et al. (2017), with minor modifications. Embryos from each mutant line were collected, observed, and phenotyped (WT-like, organless, and topsy-turvy). After eosin B staining, samples were placed in a glass cell culture dish (Nest), observed by TCS SP8 confocal microscope (Leica), and photographed at 561 nm with a 10× objective lens. To observe embryos at 1 DAP, rice florets were fixed (Anderson et al. 2017) at 6, 12, 18, 24, and 30 h after pollination, and treated as above. Dissected ovaries were placed on the slide, 400 μl 100% (v/v) methyl salicylate added, and pressed before covering with a coverslip. Images were captured using the Olympus IXplore SpinSR confocal microscope (60× objective).

Paraffin-thin section and staining was performed as described by Wu et al. (2018), with minor modifications. Embedded samples were sectioned into 6 mm slices using a Leica rotary microtome (RM2245). After deparaffinization, a 0.02% (w/v) toluidine blue staining solution was used to stain embryonic sections (30 s to 1 min). Images were captured using a Nikon microscope (Eclipse 80i).

For computed tomography (CT) scanning, mature dry rice seeds were fixed with FAA (5% glacial acetic acid, 3.7% formaldehyde, 50% alcohol, v/v) for 24 h, followed by ethanol gradient dehydration (50%, 70%, 80%, 90%, 100%, v/v, each for 15 min), staining in 100% (v/v) ethanol solution containing 1% (w/v) iodine for 6 h, followed by rinsing with 100% (v/v) ethanol and critical point drying with CO_2. An X-ray microscope (Xradia 520 Versa) was used to image seeds using a 4× objective lens, 3 μm resolution, and exposure time of 1 s.

For observations of seed germination, 250 WT and *dwt1* seeds were placed on water-immersed filter paper and incubated at 28 °C with a 16 h:8 h light:dark cycle for 5 d, and subsequently counted and photographed using a Lecia stereomicroscope (M205A).

Measurements of the transverse and longitudinal axis length of embryos at the 2 to 5 DAP stages were directly taken using LAS AF LITE 2.80 software (Lecia), with 9 typical samples of WT and topsy-turvy embryos selected for statistical analysis at each stage. As for the measurement details, before the globular embryo stage, the lengths of the transverse and longitudinal axes are directly measured by measuring the distance between the left and right and basal apical vertexes. During the 4 to 5 DAP stage, the longitudinal axis length is still measured by measuring the distance between the basal and apical points, while the transverse axis length is measured by measuring the distance from the farthest end of the left scutellum to the SAM on the right side.

RNA in situ hybridization

For mRNA in situ hybridizations, embryos were fixed in FAA as described above, on ice, and for no longer than 16 h. Probes were prepared according to Sun et al. (2021) using the DIG RNA Labelling Kit (SP6/T7; Roche). Most probe sequences were derived from published articles: *DWT1* (Wang et al. 2014); *zinc finger nuclease 1* (*ZFN1*), *ACC oxidase 1* (*ACO1*), *ERECTA-like kinase 1* (*ERECTA*), and *piriformospora indica-insensitive protein 2* (*PIP2*) (Itoh et al. 2016);

and *OsHB1*, *OsHB3*, and *OsHB4* (Itoh et al. 2008). Primers for other probes are listed in Supplementary Table S4. Pretreatment of sections, hybridization, post-hybridization treatment, and digoxigenin signal detection were performed as described (Chu et al. 2006). Images were obtained using a Nikon microscope (Eclipse 80i).

Fluorescence imaging

Embryos were prepared in 10% (w/v) sucrose as a sample buffer. Rice ovaries from transgenic plants were peeled from the glume and placed in a cell culture dish (Nest). A scalpel was used to cut the base of the ovary, which was then pressed gently to allow the embryonic tissue to slide out. For 1 to 3 DAP embryos, the surrounding tissue also had to be carefully dissected away, while embryos from 6 DAP were sectioned in the middle prior to observation. Fluorescent and bright field images were captured using a TCS SP8 confocal microscope (Leica) with solid-state argon laser, using excitation of 488 nm and emission of 505 to 525 nm for GFP, the intensity is set at 90%, with a smart gain of 800.0 V; and excitation of 514 nm and emission of 525 to 600 nm for Venus, the intensity is set at 40%, with a smart gain of 300.0 V.

Statistical analysis

Statistical analyses of all bar graphs were performed using Microsoft Excel (https://www.microsoft.com/zh-cn/microsoft-365/excel). The data are presented as mean ± SD. Image stitching and generation mainly rely on Microsoft PowerPoint (https://www.microsoft.com/zh-cn/microsoft-365/powerpoint) and Adobe Photoshop (https://www.adobe.com/products/photoshop.html) software. For the CT scan results, the original images and videos were processed and output using ORS Dragonfly (https://www.theobjects.com/dragonfly/index.html) 3D image analysis software, and the videos were annotated by the video processing software Adobe Premiere Pro (https://www.adobe.com/products/premiere.html).

Accession numbers

Sequence data can be found in the GenBank/EMBL data libraries under the following accession numbers: *DWT1* (Os01g0667400), *DWL2* (Os05g0564500), and *DWL1* (Os07g0533201).

Acknowledgments

We thank Mr. Zhijin Luo, Ms. Mingjiao Chen, and Mr. Zibo Chen (Shanghai Jiao Tong University) for rice growth; Ms. Xiaofei Chen for gene transformation. We thank the Core Facility and Service Center (CFSC) of School of Life Sciences and Biotechnology, SJTU for fluorescence imaging data collection.

Author contributions

J.T. performed research, analyzed data, and wrote the paper. W.L. designed the research project. M.S. provided suggestions. X.H. directed and participated in some experiments.

Supplementary data

The following materials are available in the online version of this article.

Supplementary Figure S1. In situ hybridization of *DWT1* in WT embryos at 1 to 4 DAP.

Supplementary Figure S2. Bioinformatic analysis of OsWOX9 sequences and distribution of DWL2 in embryos.

Supplementary Figure S3. Structures and mutations of *OsWOX9* genes.

Supplementary Figure S4. Early embryo development from 6 to 9 DAP.

Supplementary Figure S5. Serial transverse sections of WT and organ-less ($DWT1^{+/-}dwl2$) embryos at 3 DAP.

Supplementary Figure S6. DR5-VENUS signal distribution in WT, organ-less (ol), and topsy-turvy embryos.

Supplementary Figure S7. In situ hybridization of *OSH1*, *PLT1*, and *BBM1* in WT and $DWT1^{+/-}dwl2$ (organ-less) embryos at 3 DAP.

Supplementary Figure S8. Morphological comparison of embryos and seeds.

Supplementary Figure S9. Further embryo morphologies observed via clear staining.

Supplementary Table S1. Genotype analysis of the *OsWOX9* clade multiple mutants.

Supplementary Table S2. Abnormal embryos with *OsWOX9* clade gene mutations.

Supplementary Table S3. Phenotypes of *dwt1* and WT seeds after 5 d of germination.

Supplementary Table S4. Primers used in this study.

Supplementary Video S1. CT scan of wild type mature embryo. em, embryo; en, endosperm; RAM, root apical meristem; SAM, shoot apical meristem; WT, wild type.

Supplementary Video S2. CT scan of topsy-turvy mature embryo. em, embryo; en, endosperm; RAM, root apical meristem; SAM, shoot apical meristem.

Funding

This work was supported by funds from the National Natural Science Foundation of China (32370344).

Conflict of interest statement. None declared.

Data availability

The data underlying this article are available in the article and in its online supplementary material.

References

Aida M, Beis D, Heidstra R, Willemsen V, Blilou I, Galinha C, Nussaume L, Noh YS, Amasino R, Scheres B. The PLETHORA genes mediate patterning of the Arabidopsis root stem cell niche. *Cell*. 2004:119(1):109–120. https://doi.org/10.1016/j.cell.2004.09.018

Anderson SN, Johnson CS, Chesnut J, Jones DS, Khanday I, Woodhouse M, Li C, Conrad LJ, Russell SD, Sundaresan V. The zygotic transition is initiated in unicellular plant zygotes with asymmetric activation of parental genomes. *Dev Cell*. 2017:43(3):349–358.e344. https://doi.org/10.1016/j.devcel.2017.10.005

Armenta-Medina A, Gillmor CS. Genetic, molecular and parent-of-origin regulation of early embryogenesis in flowering plants. *Curr Top Dev Biol*. 2019:131:497–543. https://doi.org/10.1016/bs.ctdb.2018.11.008

Armenta-Medina A, Lepe-Soltero D, Xiang D, Datla R, Abreu-Goodger C, Gillmor CS. *Arabidopsis thaliana* miRNAs promote embryo pattern formation beginning in the zygote. *Dev Biol*. 2017:431(2):145–151. https://doi.org/10.1016/j.ydbio.2017.09.009

Bayer M, Nawy T, Giglione C, Galli M, Meinnel T, Lukowitz W. Paternal control of embryonic patterning in *Arabidopsis thaliana*. *Science*. 2009:323(5920):1485–1488. https://doi.org/10.1126/science.1167784

Breuninger H, Rikirsch E, Hermann M, Ueda M, Laux T. Differential expression of WOX genes mediates apical–basal axis formation in the Arabidopsis embryo. *Dev Cell*. 2008:14(6):867–876. https://doi.org/10.1016/j.devcel.2008.03.008

Chen J, Lausser A, Dresselhaus T. Hormonal responses during early embryogenesis in maize. *Biochem Soc Trans*. 2014:42(2):325–331. https://doi.org/10.1042/BST20130260

Cheng S, Huang Y, Zhu N, Zhao Y. The rice WUSCHEL-related homeobox genes are involved in reproductive organ development, hormone signaling and abiotic stress response. *Gene*. 2014:549(2):266–274. https://doi.org/10.1016/j.gene.2014.08.003

Chu H, Qian Q, Liang W, Yin C, Tan H, Yao X, Yuan Z, Yang J, Huang H, Luo D, *et al*. The floral organ number4 gene encoding a putative ortholog of Arabidopsis CLAVATA3 regulates apical meristem size in rice. *Plant Physiol*. 2006:142(3):1039–1052. https://doi.org/10.1104/pp.106.086736

Dresselhaus T, Jurgens G. Comparative embryogenesis in angiosperms: activation and patterning of embryonic cell lineages. *Annu Rev Plant Biol*. 2021:72(1):641–676. https://doi.org/10.1146/annurev-arplant-082520-094112

Fang F, Ye S, Tang J, Bennett MJ, Liang W. DWT1/DWL2 act together with OsPIP5K1 to regulate plant uniform growth in rice. *New Phytol*. 2020:225(3):1234–1246. https://doi.org/10.1111/nph.16216

Friml J, Vieten A, Sauer M, Weijers D, Schwarz H, Hamann T, Offringa R, Jurgens G. Efflux-dependent auxin gradients establish the apical–basal axis of Arabidopsis. *Nature*. 2003:426(6963):147–153. https://doi.org/10.1038/nature02085

Hamann T, Benkova E, Baurle I, Kientz M, Jurgens G. The Arabidopsis BODENLOS gene encodes an auxin response protein inhibiting MONOPTEROS-mediated embryo patterning. *Genes Dev*. 2002:16-(13):1610–1615. https://doi.org/10.1101/gad.229402

Hardtke CS, Berleth T. The Arabidopsis gene MONOPTEROS encodes a transcription factor mediating embryo axis formation and vascular development. *EMBO J*. 1998:17(5):1405–1411. https://doi.org/10.1093/emboj/17.5.1405

Hendelman A, Zebell S, Rodriguez-Leal D, Dukler N, Robitaille G, Wu X, Kostyun J, Tal L, Wang P, Bartlett ME, *et al*. Conserved pleiotropy of an ancient plant homeobox gene uncovered by cis-regulatory dissection. *Cell*. 2021:184(7):1724–1739.e1716. https://doi.org/10.1016/j.cell.2021.02.001

Hiei Y, Ohta S, Komari T, Kumashiro T. Efficient transformation of rice (*Oryza sativa* L.) mediated by Agrobacterium and sequence analysis of the boundaries of the T-DNA. *Plant J*. 1994:6(2):271–282. https://doi.org/10.1046/j.1365-313X.1994.6020271.x

Huang X, Peng X, Sun MX. OsGCD1 is essential for rice fertility and required for embryo dorsal-ventral pattern formation and endosperm development. *New Phytol*. 2017:215(3):1039–1058. https://doi.org/10.1111/nph.14625

Ishimoto K, Sohonahra S, Kishi-Kaboshi M, Itoh JI, Hibara KI, Sato Y, Watanabe T, Abe K, Miyao A, Nosaka-Takahashi M, *et al*. Specification of basal region identity after asymmetric zygotic division requires mitogen-activated protein kinase 6 in rice. *Development*. 2019:146(13):dev176305. https://doi.org/10.1242/dev.176305

Itoh J, Hibara K, Sato Y, Nagato Y. Developmental role and auxin responsiveness of class III homeodomain leucine zipper gene family members in rice. *Plant Physiol*. 2008:147(4):1960–1975. https://doi.org/10.1104/pp.108.118679

Itoh J, Nonomura K, Ikeda K, Yamaki S, Inukai Y, Yamagishi H, Kitano H, Nagato Y. Rice plant development: from zygote to spikelet. *Plant Cell Physiol*. 2005:46(1):23–47. https://doi.org/10.1093/pcp/pci501

Itoh J, Sato Y, Sato Y, Hibara K, Shimizu-Sato S, Kobayashi H, Takehisa H, Sanguinet KA, Namiki N, Nagamura Y. Genome-wide analysis of spatiotemporal gene expression patterns during early embryogenesis in rice. *Development*. 2016:143(7):1217–1227. https://doi.org/10.1242/dev.123661

Ito M, Sentoku N, Nishimura A, Hong SK, Sato Y, Matsuoka M. Position dependent expression of GL2-type homeobox gene, Roc1: significance for protoderm differentiation and radial pattern formation in early rice embryogenesis. *Plant J*. 2002:29(4):497–507. https://doi.org/10.1046/j.1365-313x.2002.01234.x

Izhaki A, Bowman JL. KANADI and class III HD-Zip gene families regulate embryo patterning and modulate auxin flow during embryogenesis in Arabidopsis. *Plant Cell*. 2007:19(2):495–508. https://doi.org/10.1105/tpc.106.047472

Jiang YT, Tang RJ, Zhang YJ, Xue HW, Ferjani A, Luan S, Lin WH. Two tonoplast proton pumps function in Arabidopsis embryo development. *New Phytol*. 2020:225(4):1606–1617. https://doi.org/10.1111/nph.16231

Kamiya N, Nagasaki H, Morikami A, Sato Y, Matsuoka M. Isolation and characterization of a rice WUSCHEL-type homeobox gene that is specifically expressed in the central cells of a quiescent center in the root apical meristem. *Plant J*. 2003:35(4):429–441. https://doi.org/10.1046/j.1365-313X.2003.01816.x

Khanday I, Skinner D, Yang B, Mercier R, Sundaresan V. A male-expressed rice embryogenic trigger redirected for asexual propagation through seeds. *Nature*. 2019:565(7737):91–95. https://doi.org/10.1038/s41586-018-0785-8

Li P, Xue H. Structural characterization and expression pattern analysis of the rice PLT gene family. *Acta Biochim Biophys Sin (Shanghai)*. 2011:43(9):688–697. https://doi.org/10.1093/abbs/gmr068

Lian G, Ding Z, Wang Q, Zhang D, Xu J. Origins and evolution of WUSCHEL-related homeobox protein family in plant kingdom. *ScientificWorldJournal*. 2014:2014:534140. https://doi.org/10.1155/2014/534140

Lippman ZB, Cohen O, Alvarez JP, Abu-Abied M, Pekker I, Paran I, Eshed Y, Zamir D. The making of a compound inflorescence in tomato and related nightshades. *PLoS Biol*. 2008:6(11):e288. https://doi.org/10.1371/journal.pbio.0060288

Lukowitz W, Roeder A, Parmenter D, Somerville C. A MAPKK kinase gene regulates extra-embryonic cell fate in Arabidopsis. *Cell*. 2004:166(1):109–119. https://doi.org/10.1016/S0092-8674(03)01067-5

Moller B, Weijers D. Auxin control of embryo patterning. *Cold Spring Harb Perspect Biol*. 2009:1(5):a001545. https://doi.org/10.1101/cshperspect.a001545

Nagasaki H, Itoh J, Hayashi K, Hibara K, Satoh-Nagasawa N, Nosaka M, Mukouhata M, Ashikari M, Kitano H, Matsuoka M, *et al*. The small interfering RNA production pathway is required for shoot meristem initiation in rice. *Proc Natl Acad Sci U S A*. 2007:104(37):14867–14871. https://doi.org/10.1073/pnas.0704339104

Nardmann J, Zimmermann R, Durantini D, Kranz E, Werr W. WOX gene phylogeny in Poaceae: a comparative approach addressing leaf and embryo development. *Mol Biol Evol*. 2007:24(11):2474–2484. https://doi.org/10.1093/molbev/msm182

Nishimura A, Ito M, Kamiya N, Sato Y, Matsuoka M. OsPNH1 regulates leaf development and maintenance of the shoot apical meristem in rice. *Plant J*. 2002:30(2):189–201. https://doi.org/10.1046/j.1365-313X.2002.01279.x

Palovaara J, de Zeeuw T, Weijers D. Tissue and organ initiation in the plant embryo: a first time for everything. *Annu Rev Cell Dev Biol*. 2016:32(1):47–75. https://doi.org/10.1146/annurev-cellbio-111315-124929

Palovaara J, Hallberg H, Stasolla C, Hakman I. Comparative expression pattern analysis of WUSCHEL-related homeobox 2 (WOX2)

and WOX8/9 in developing seeds and somatic embryos of the gymnosperm *Picea abies*. *New Phytol*. 2010:188(1):122–135. https://doi.org/10.1111/j.1469-8137.2010.03336.x

Prigge MJ, Otsuga D, Alonso JM, Ecker JR, Drews GN, Clark SE. Class III homeodomain-leucine zipper gene family members have overlapping, antagonistic, and distinct roles in Arabidopsis development. *Plant Cell*. 2005:17(1):61–76. https://doi.org/10.1105/tpc.104.026161

Robert Hélène S, Grones P, Stepanova Anna N, Robles Linda M, Lokerse Annemarie S, Alonso Jose M, Weijers D, Friml J. Local auxin sources orient the apical–basal axis in Arabidopsis embryos. *Curr Biol*. 2013:23(24):2506–2512. https://doi.org/10.1016/j.cub.2013.09.039

Roodbarkelari F, Groot EP. Regulatory function of homeodomain-leucine zipper (HD-ZIP) family proteins during embryogenesis. *New Phytol*. 2017:213(1):95–104. https://doi.org/10.1111/nph.14132

Sato Y, Hong S, Tagiri A. A rice homeobox gene, OSH1, is expressed before organ differentiation in a specific region during early embryogenesis. *Proc Natl Acad Sci U S A*. 1996:93(15):8117–8122. https://doi.org/10.1073/pnas.93.15.8117

Sazuka T, Kamiya N, Nishimura T, Ohmae K, Sato Y, Imamura K, Nagato Y, Koshiba T, Nagamura Y, Ashikari M, *et al.* A rice tryptophan deficient dwarf mutant, tdd1, contains a reduced level of indole acetic acid and develops abnormal flowers and organless embryos. *Plant J*. 2009:60(2):227–241. https://doi.org/10.1111/j.1365-313X.2009.03952.x

Schorderet M, Duvvuru Muni RR, Fiebig A, Reinhardt D. Deregulation of MADS-box transcription factor genes in a mutant defective in the WUSCHEL-LIKE HOMEOBOX gene EVERGREEN of *Petunia hybrida*. *Plant Signal Behav*. 2018:13(6):e1471299. https://doi.org/10.1080/15592324.2018.1471299

Smith ZR, Long JA. Control of Arabidopsis apical–basal embryo polarity by antagonistic transcription factors. *Nature*. 2010:464(7287):423–426. https://doi.org/10.1038/nature08843

Sun L, Yuan Z, Wang D, Li J, Shi J, Hu Y, Yu J, Chen X, Chen S, Liang W, *et al.* Carbon Starved Anther modulates sugar and ABA metabolism to protect rice seed germination and seedling fitness. *Plant Physiol*. 2021:187(4):2405–2418. https://doi.org/10.1093/plphys/kiab391

ten Hove CA, Lu KJ, Weijers D. Building a plant: cell fate specification in the early Arabidopsis embryo. *Development*. 2015:142(3):420–430. https://doi.org/10.1242/dev.111500

Ueda M, Aichinger E, Gong W, Groot E, Verstraeten I, Vu LD, Smet ID, Higashiyama T, Umeda M, Laux T. Transcriptional integration of paternal and maternal factors in the Arabidopsis zygote. *Genes Dev*. 2017:31(6):617–627. https://doi.org/10.1101/gad.292409.116

Wang L, Yuan J, Ma Y, Jiao W, Ye W, Yang DL, Yi C, Chen ZJ. Rice interploidy crosses disrupt epigenetic regulation, gene expression, and seed development. *Mol Plant*. 2018:11(2):300–314. https://doi.org/10.1016/j.molp.2017.12.006

Wang W, Li G, Zhao J, Chu H, Lin W, Zhang D, Wang Z, Liang W. Dwarf Tiller1, a Wuschel-related homeobox transcription factor, is required for tiller growth in rice. *PLoS Genet*. 2014:10(3):e1004154. https://doi.org/10.1371/journal.pgen.1004154

Wendrich JR, Weijers D. The Arabidopsis embryo as a miniature morphogenesis model. *New Phytol*. 2013:199(1):14–25. https://doi.org/10.1111/nph.12267

Wu D, Liang W, Zhu W, Chen M, Ferrandiz C, Burton RA, Dreni L, Zhang D. Loss of LOFSEP transcription factor function converts spikelet to leaf-like structures in rice. *Plant Physiol*. 2018:176(2):1646–1664. https://doi.org/10.1104/pp.17.00704

Wu X, Chory J, Weigel D. Combinations of WOX activities regulate tissue proliferation during Arabidopsis embryonic development. *Dev Biol*. 2007:309(2):306–316. https://doi.org/10.1016/j.ydbio.2007.07.019

Yang J, Yuan Z, Meng Q, Huang G, Perin C, Bureau C, Meunier AC, Ingouff M, Bennett MJ, Liang W, *et al.* Dynamic regulation of auxin response during rice development revealed by newly established hormone biosensor markers. *Front Plant Sci*. 2017:8:256. https://doi.org/10.3389/fpls.2017.00256

Yi J, Lee YS, Lee DY, Cho MH, Jeon JS, An G. OsMPK6 plays a critical role in cell differentiation during early embryogenesis in *Oryza sativa*. *J Exp Bot*. 2016:67(8):2425–2437. https://doi.org/10.1093/jxb/erw052

Zhang H, Zhang J, Wei P, Zhang B, Gou F, Feng Z, Mao Y, Yang L, Zhang H, Xu N, *et al.* The CRISPR/Cas9 system produces specific and homozygous targeted gene editing in rice in one generation. *Plant Biotechnol J*. 2014:12(6):797–807. https://doi.org/10.1111/pbi.12200

Zhang MM, Wu H, Su J, Wang H, Zhu Q, Liu Y, Xu J, Lukowitz W, Zhang S. Maternal control of embryogenesis by MPK6 and its upstream MKK4/MKK5 in Arabidopsis. *Plant J*. 2017:92(6):1005–1019. https://doi.org/10.1111/tpj.13737

Zhang ZJ, Tucker E, Hermann M, Laux T. A molecular framework for the embryonic initiation of shoot meristem stem cells. *Dev Cell*. 2017:40(3):264–277.e264. https://doi.org/10.1016/j.devcel.2017.01.002